ELSEVIER

Biochimica et Biophysica Acta 1370 (1998) 17–30

BIOCHIMICA ET BIOPHYSICA ACTA
BBA

Probing DNA–cationic lipid interactions with the fluorophore trimethylammonium diphenyl-hexatriene (TMADPH) [1]

Danielle Hirsch-Lerner, Yechezkel Barenholz *

Department of Biochemistry, Hadassah Medical School, The Hebrew University, P.O. Box 12272, Jerusalem 91120, Israel

Received 15 July 1997; revised 29 September 1997; accepted 2 October 1997

Abstract

The aim of this study is to get a better understanding of DNA–cationic lipid complex formation and its characterization through the properties of the lipid assembly, using fluorescent probes known to have different locations in the vesicle bilayer, 1,6-diphenylhexa-1,3,5-triene (DPH) and 1-(4-trimethylammoniumphenyl)-6-phenyl-1,3,5-hexatriene (TMADPH). The location of these two fluorescent probes in the membrane differs; the positive charge of TMADPH is localized close to the water/lipid interface and its fluorophore is present in the upper part of the acyl chain region while DPH (lacking polar group) is embedded deeper in the hydrophobic part of the bilayer. Unilamellar vesicles (~100 nm size) composed of *N*-(1-(2,3-dioleoyloxy)-propyl)-*N*,*N*,*N*-trimethylammonium chloride (DOTAP) and 1,2-dioleoyl-*sn*-glycero-3-phosphoethanolamine (DOPE) as a helper lipid (at 1:1 mole ratio) were used as a model of cationic liposomes. Both linear and circular DNA gave almost identical results. DNA^-/L^+ (mole charge ratio of DNA negatively-charged phosphate to positively-charged lipid) ratios have large effects on the measured parameters. The effects monitored through TMADPH are much more striking than those obtained through the use of DPH, suggesting that the major DNA–lipid interaction occurs at the lipid/water interface. The fact that DNA induced much larger changes in TMADPH fluorescence intensity in H_2O than in D_2O suggests that the changes in the exposure of TMADPH to water and solvent relaxation effects are involved in the interaction. At $DNA^-/L^+ \geq 1$, fluorescence intensity increased concomitantly with a small increase in TMADPH fluorescence anisotropy without much affect in the size of the complex. At $DNA^-/L^+ < 0.6$, fluorescence quenching proportional to DNA^-/L^+ occurred, as well as a large increase in TMADPH fluorescence anisotropy and in complex size. These results suggest that at low DNA^-/L^+, negatively-charged DNA condenses positively-charged lipid headgroups, thereby inducing formation of lipid-ordered domains. This phase separation results in membrane defects at the lipid/water

Abbreviations: cryo-TEM, cryo-transmission electron microscopy; DC-Chol, 3β-[*N*-(*N*′,*N*′-dimethylaminoethane)-carbamoyl]-cholesterol; DMPC, 1,2-dimyristoyl-*sn*-glycero-3-phosphocholine; DNA^-/L^+, mole charge ratio of DNA negatively-charged phosphate to positively-charged lipid; DOPC, 1,2-dioleoyl-*sn*-glycero-3-phosphocholine; DOPE, 1,2-dioleoyl-*sn*-glycero-3-phosphoethanolamine; DOTAP, *N*-(1-(2,3-dioleoyloxy)propyl)-*N*,*N*,*N*-trimethylammonium chloride; DOTMA, *N*-(1-(2,3-dioleyloxy)propyl)-*N*,*N*,*N*-trimethylammonium chloride; DPH, 1,6-diphenylhexa-1,3,5-triene; DSC, differential scanning calorimetry; Hepes, *N*-(2-hydroxyethyl)piperazine-*N*′-(2-ethanesulfonic acid); L^+, positively charged lipid; LUV, large (≥ 100 nm) unilamellar vesicles; MLV, multilamellar vesicles; PCS, photon correlation spectroscopy ; PC, phosphatidylcholine; PE, phosphatidylethanolamine; *r*, fluorescence anisotropy; TMADPH, 1-(4-trimethylammoniumphenyl)-6-phenyl-1,3,5-hexatriene.

* Corresponding author. Fax: 972 2 6411663; E-mail: yb@cc.huji.ac.il

[1] A preliminary report of this study was presented at the ''Artificial Self-assembling Systems for Gene Transfer'' Conferences of the Cambridge Healthtech Institute, September 28–29, 1995, Wakefield, MA, and November 17–18, 1996, Coronado, CA.

PII S0005-2736(97)00239-3

interface and increased exposure of the hydrophobic upper parts of the acyl chains to water, as indicated by the quenching of TMADPH. This leads to instability and aggregation/fusion of the DNA–lipid complexes. On the other hand, at $DNA^-/L^+ \geq 1$, the condensing effect is smaller, involving homogeneous lateral condensation of all the lipids, leading to a reduction in water content near the probe, and the DNA–lipid complexes are relatively small and stable. © 1998 Elsevier Science B.V.

Keywords: Cationic liposome; Transfection; Cationic lipid DNA complex; Hydration; Domain

1. Introduction

Cationic lipids have been widely used in many different kinds of eukaryotic cells for gene delivery [1–7]. This use of lipid amphiphiles for transfection is referred to as lipofection. The positively-charged liposomes interact spontaneously and strongly with the negatively-charged nucleic acids, without requiring the DNA passive entrapment which is necessary for gene delivery by neutral or anionic liposomes. The cationic lipid–polynucleotide complexes present several major advantages over retroviral vectors, including the absence of viral DNA, no constraint on DNA size, protection of DNA from degradation, and ability to target recombinant genes to specific cells. It was suggested that the main barriers to successful lipofection by cationic lipid–polynucleotide complexes involve the following: complex polymorphism, entry of the complex into the cell, its escape from the endosome, dissociation of the polynucleotide from the cationic lipid, and its entry into the nucleus [8].

DOTMA (*N*-(1-(2,3-dioleyloxy)propyl)-*N*,*N*,*N*-trimethylammonium chloride) was the first cationic lipid developed. To optimize transfection in cell culture, DOTMA was used in combination with a helper zwitterionic lipid, DOPE (1,2-dioleoyl-*sn*-glycero-3-phosphoethanolamine) [7]. This combination is sold as Lipofectin™ (Life Technologies, Gaithersburg, MD). The pure DOPE has the ability to adopt the inverted hexagonal II phase, which may improve the transfection process [5–7]. In addition, DOPE, possibly through induction of fusion, has been suggested to be an important part of the delivery path of DNA through the cell membrane [6,9]; DOPE also reduces the uptake by lysosomes which lowers lipofection efficacy [10].

DOTAP (*N*-(1-(2,3-dioleoyloxy)propyl)-*N*,*N*,*N*-trimethylammonium chloride) was synthesized as an alternative to DOTMA and is commercially available from Boehringer, Mannheim, Germany in liposome formulation as 'transfection-reagent'. The advantage of DOTAP over DOTMA is that it has an ester group, which is biodegradable, instead of an ether group, which is not. This advantage raises the question of the chemical stability of DOTAP during preparation and storage. However, DOTAP was used successfully in vitro and in vivo for lipofection [3,11–13]. Many other monovalent cationic lipids were synthesized, such as DMRIE (1,2-dimyristyloxypropyl-3-dimethyl-hydroxyethyl ammonium bromide) [14,15] and DC-Chol (3β-[N-(*N′*,*N′*-dimethylamino-ethane)-carbamoyl]-cholesterol) [4], in order to improve lipofection efficiency and lower toxicity.

In spite of the extensive use of cationic lipids for DNA delivery, many aspects of the DNA complexation are still not clear, and interpretations of similar results obtained by similar methods by different laboratories differ extensively. This is exemplified by comparing the pioneer detailed biophysical study of Minsky and coworkers [16,17] on the complexation between DNA and DOTMA:DOPE (1:1 mole ratio) with a recent study [18] using four cationic lipids (differing in having 1–4 positive charges/molecule), each in liposomes containing 50 mol% DOPE. Both studies have similar experimental results. They agreed on the interpretation that the DNA induced lipid mixing concomitant with DNA condensation, and that the increase in complex size occurred mainly at $DNA^-/L^+ \leq 0.6$. They disagreed on whether the DNA in the complex is encapsulated by a lipid bilayer or not. Minsky and coworkers favor DNA encapsulation at DNA^-/L^+ charge ratio slightly lower than 1.0 [16,17], while Eastman et al. [18] claim that throughout all the range of DNA^-/L^+ charge ratio there is no DNA encapsulation and the majority of the DNA is bound to the lipids in the complex without being coated. It becomes obvious

that some of the basic properties of the complexes involving DNA and cationic lipids, such as electrical zeta potential, size, and structure, are strongly dependent on the DNA^-/L^+ charge ratio [7,16–18]. It is also clear that the dominant forces leading to complex formation are electrostatic in nature. However, the exact mechanism of the complexation and how it is affected by the DNA^-/L^+ charge ratio are still missing. This study is aimed to fill part of this gap, especially the relation between the effect of lipid–DNA complexation on the lateral organization of the lipids and on the macroscopic structure of the complex.

2. Materials and methods

2.1. Materials

2.1.1. Linear and circular DNA preparation

Highly polymerized calf thymus DNA (type I, Sigma) was dissolved in 20 mM Tris buffer, pH 7.5, and then sonicated for 4×30 s with a Microson Ultrasonic Cell Disruptor (Heat Systems–Ultrasonics, Plainview, NY). The sonicated DNA was separated on a Sephacryl S-400 (Pharmacia LKB Biotechnology) column eluted with 20 mM Tris (pH 7.5), 0.25 M NaCl. Fractions of 6 ml were collected and the DNA's size was estimated by means of 1% agarose gel electrophoresis. The size collected was $\approx$ 2–4 kbp. Afterwards, DNA was concentrated by ethanol precipitation, followed by centrifugation at 15 000 rpm for 30 min at 4°C. Then the polynucleotides were resuspended in 20 mM Hepes buffer (pH 7.4) and 10 mM NaCl. DNA concentration was determined spectrophotometrically at 260 nm according to the relationship: absorbance of $1.00 = 40\ \mu g$ DNA/ml. This determination agreed well with DNA phosphate determination [19].

The S16 hGH plasmid ($\sim$ 5 kbp) was obtained from Dr. O. Meyuhas of our department [20]. The plasmid DNA was isolated using a QIAGEN Plasmid Kit (QIAGEN GmbH, Hilden, Germany).

2.1.2. Liposome preparation

DOTAP, DOPE, and DOPC were purchased from Avanti Polar Lipids (Alabaster, AL). The fluorescent probes 1-(4-trimethylammoniumphenyl)-6-phenyl-1,3,5-hexatriene, *p*-toluenesulfonate (TMADPH) and 1,6-diphenylhexa-1,3,5-triene (DPH) were obtained from Molecular Probes (Eugene, OR).

Fluorescent-labeled large unilamellar vesicles (LUV) were prepared by mixing chloroform solutions of the different lipids with 1 mol of fluorophore per 200 mol of lipids. TMADPH was dissolved in tetrahydrofuran : ethanol (1 : 1, v/v), and DPH, in tetrahydrofuran. The solvents were evaporated by a rotary evaporator until a thin, dried lipid film was formed. *tert*-Butanol was added to co-dissolve the lipids and the fluorophores, and the mixture was freeze-dried and stored at -20°C, protected from light, until further use. The lyophilized 'cake' was hydrated with the desired aqueous phase in 20 mM Hepes buffer (pH 7.4) and 10 mM NaCl at a concentration of lipid of 4 mM or 31 mM, and the suspension was vortexed to produce multilamellar vesicles (MLV). The MLV were extruded stepwise through 0.4 μm and then 0.1 μm polycarbonate filters (Poretics, Livermore, CA) mounted in the extruder Liposofast (Avestin, Ottawa, Canada) to form LUV. An odd number of passages (11 or 15) were carried out to avoid the presence of MLV which might not cross through the filter [21].

2.2. Fluorescence experiments

Fluorescence measurements were performed on a Perkin Elmer LS 50B luminescence spectrometer using a 1 cm light path cell. An aliquot of fluorescent-labeled liposomes was diluted with 1 ml Hepes buffer to the desired concentration. The fluorescence intensity of the fluorescent-labeled liposomes without DNA (F_0) was measured (excitation at 360 nm and emission at 430 nm). The fluorescence intensity (F) was measured 5 min after the addition of DNA. Every experiment was repeated at least twice (and in most cases more than three times) with good reproducibility.

The fluorescence anisotropy (r) measurements for TMADPH were also done on this spectrofluorometer. First, the factor G was estimated by computation, correcting for optical and electronic differences in the parallel and perpendicular channels. Then r was measured. All data were corrected for light scattering as described by Borenstain and Barenholz [22].

2.3. Turbidity measurements

Turbidity was measured as light scattering at 90° using the above spectrofluorometer at both emission and excitation wavelength of 600 nm, with an attenuation of 1%.

2.4. Size distribution analysis

Size distribution was determined by photon correlation spectroscopy (PCS) using a Coulter N4SD submicron particle analyzer and size distribution processor analysis (Coulter Electronics, Luton, UK) [29]. These measurements were confirmed by cryo-transmission electron microscopy (cryo-TEM) [23].

2.5. Differential scanning calorimetry (DSC) measurements

The ratio of bound water molecules to lipid molecules was calculated from the heat capacity profiles of a water–lipid mixture by means of a Mettler TA4000 differential scanning calorimeter [24]. The samples were scanned from -30°C to $+30$°C at a rate of 2°C/min. The ice–water fusion heat enthalpy (ΔH_{fu}) was calculated to be 320 J/g. The temperature of maximum change in specific heat capacity (ΔC_p) during the gel-to-liquid-crystalline main phase transition (T_m) of DOTAP was also obtained through these measurements at conditions of excess water.

3. Results

3.1. Characterization of liposomes and DNA–lipid complexes

Mixtures composed of a 1 : 1 mol ratio of DOTAP/DOPE, DOTAP/DOPC, or DOPC/DOPE, when hydrated and extruded through polycarbonate filters of 100 nm pore size, form LUV having unimodal size distribution of similar mean size ($\sim$ 100 nm) (Table 1) and therefore similar vesicle curvature. Cryo-TEM of DOTAP/DOPE LUV, performed by Y. Talmon and M. Goldraich, of the Department of Chemical Engineering, Technion, Haifa, Israel, confirmed the PCS measurements and showed that almost all the vesicles are unilamellar.

TMADPH steady-state fluorescence anisotropy of the three vesicle systems ($r \sim 0.2$, Section 4 below), and T_m values (Table 1) indicate that at room temperature these systems are in the fluid phase [28].

We found that 8.7 mol of water per mole DOTAP were measured as tightly bound water (Table 1), compared to 11 moles of water per mole of egg PC and dimyristoyl PC, in agreement with Katz and Diamond [27]. The emission fluorescence intensity of TMADPH in LUV of the three compositions described above had identical spectral shapes for both excitation and emission. However, the specific fluorescence emission intensity of TMADPH obtained in DOPC/DOPE was 1.5- and 1.7-fold higher than in

Table 1
Properties of lipids and liposomes used in this study

Lipid/liposomes	T_m (°C)	Liposome size (mean $\pm$ SD), nm	TMADPH specific fluorescence[c]	Bound water[d]
DOTAP	-11.9[a]	ND	ND	8.7[a]
DOPE	-16.0[b]	ND	ND	~ 3.0[e]
DOPC	-19.0[b]	ND	ND	11.0[f]
DOTAP/DOPE 1 : 1	ND	103 ± 27	198	ND
DOTAP/DOPC 1 : 1	ND	108 ± 28	176	ND
DOPC/DOPE 1 : 1	ND	133 ± 52	294	ND

[a]This work.
[b]Measured on MLV [25].
[c]Lipid concentration was 0.8 mM.
[d]Moles of water per mole of lipid; measured on MLV.
[e]See [26].
[f]Our measurements were done on DMPC and egg PC and agreed with those of Katz and Diamond [27].
ND = No data.

Table 2
Size and specific turbidity of DOTAP/DOPE/TMADPH and DOTAP/DOPE/TMADPH liposomes before and after complexation with DNA

Liposome type	Ratio DNA^-/L^+	Size distribution (mean + SD), nm	Specific turbidity
DOTAP/DOPE 1:1	0.00	103 ± 27	2.6[a]/0.59[b]
DOTAP/DOPE 1:1	0.44	527.7 ± 162.9[c]	20.58[a]
DOTAP/DOPE 1:1	5.70	116.0 ± 11	1.35[b]
DOPE/DOPC 1:1	0.00	133.0 ± 52	5.32[a]
DOPE/DOPC 1:1	0.44	126.0 ± 31	5.39[a]

[a] Measured for 0.8 μmol lipid/ml buffer with slits Ex = Em = 2.5.
[b] Measured for 0.08 μmol lipid/ml buffer with slits Ex = Em = 5 (for details see Section 2).
[c] Very broad distribution.

DOTAP/DOPE or DOTAP/DOPC, respectively (Table 1).

Along with the formation of DOTAP/DOPE/TMADPH/DNA complexes, an augmentation in the specific turbidity was detected in the range of DNA^-/L^+ ratios < 0.6, reaching an 8-fold increase at $DNA^-/L^+ = 0.44$ (Table 2). The mean size of lipid–DNA complexes ($DNA^-/L^+ = 0.44$) as determined by PCS was about four times that of the LUV in the absence of DNA. The size increase was inde-

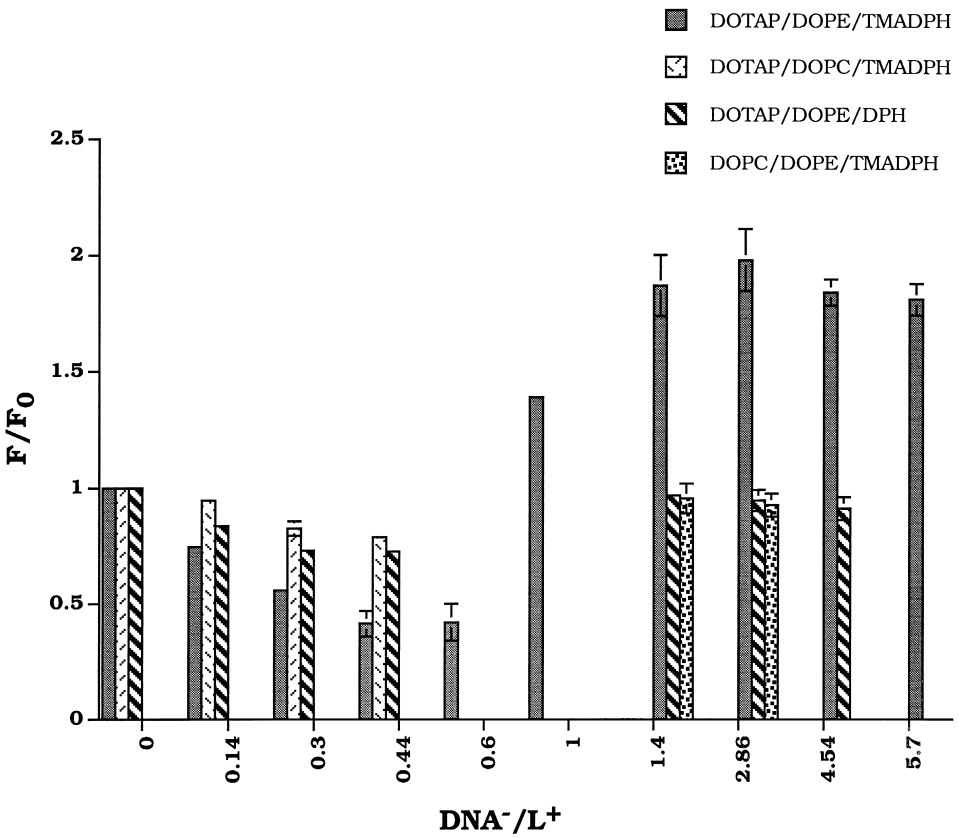

Fig. 1. Effect of mole charge ratio of DNA^-/L^+ on relative fluorescence intensity of various liposomes labeled with either TMADPH or DPH. Lipid concentrations were 0.78 mM for the range of DNA^-/L^+ from 0 to 1 and 0.08 mM for the range of DNA^-/L^+ from 1 to 5.7. Each point has a SD which can be observed only when the value is large enough to be visible.

pendent of the presence of fluorophore. At $DNA^-/L^+ = 5.7$, no change in size (PCS) and a 2-3-fold increase in the specific turbidity were observed when DNA was added to DOTAP/DOPE/TMADPH liposomes. Size and specific turbidity of DOPC/DOPE LUV were unaffected by the addition of DNA (for more details see Section 3.6).

3.2. Effect of TMADPH and DPH quenching in Hepes buffer

We used either TMADPH or DPH present in the vesicle bilayer to follow the formation of the complexes between DOTAP/DOPE vesicles and DNA. The changes in fluorescence intensities during the addition of increasing amounts of DNA to a given concentration of fluorescent-labeled liposomes are presented in Fig. 1. Two ranges of DNA^-/L^+ (0 to 0.6 and 1 to 5.7) were studied. While at a DNA^-/L^+ ratio of < 0.6, DNA induces TMADPH quenching, at a DNA^-/L^+ ratio of ≥ 1, the fluorescence intensity of TMADPH was enhanced. This increase in F/F_0 reached a plateau of about 1.5–2.0 at the DNA^-/L^+ ratio range between 1.4 and 5.7. Furthermore, at $DNA^-/L^+ = 1$, the same fluorescence intensity increases were observed for the two different L^+ concentrations, 0.39 mM and 0.04 mM (not shown in Fig. 1). Therefore, the DNA^-/L^+ ratio rather than the absolute concentration of the DNA determines the changes in TMADPH fluorescence intensity. The degree of TMADPH quenching reached when DOTAP/DOPC liposomes were used was significantly lower ($F/F_0 = 0.79$) than with DOTAP/DOPE liposomes ($F/F_0 = 0.42$). Similar fluorescence quenching occurred with plasmid DNA and linear DNA (Fig. 2), suggesting that these two forms of DNA interact similarly with the cationic lipid assemblies. No such changes in F/F_0 occurred when the cationic liposomes were labeled with DPH. Experiments in the range of DNA^-/L^+ ratios < 0.6 are detailed in Fig. 2. A plateau of 60% quenching was reached at $DNA^-/L^+ = 0.44$ when DNA was added to DOTAP/DOPE/TMADPH liposomes; at this point there was 560 μg of total lipids to 56 μg of DNA. This 10:1 weight ratio of lipid to DNA was frequently used in the in vitro transfection experiments (i.e., Leventis and Silvius [3], Nabel et al. [29]). Fig. 2 describes titration of labeled liposomes

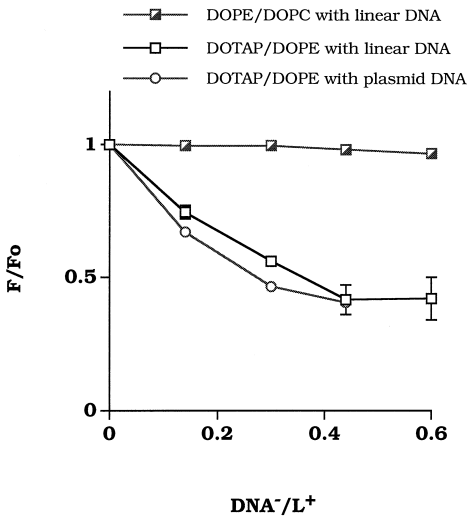

Fig. 2. Effect of DNA (linear or plasmid) on relative fluorescence intensity of various liposomes containing the fluorescent probe TMADPH. Lipid concentration was 0.78 mM. Each point has a SD which can be observed only when the value is large enough to be visible.

left unreacted in the reaction by DNA, indicating that at a DNA^-/L^+ ratio in the range of 0.44–0.6, DOTAP/DOPE liposomes interact with DNA. Controls of DOPE/DOPC/TMADPH liposomes were tested (Fig. 1 and Fig. 2), and both quenching and enhancement were not observed, indicating that quenching and enhancement of TMADPH require the presence of a cationic lipid in the liposomes.

In addition, when the order of adding the reagents was reversed and DOTAP/DOPE/TMADPH liposomes were added to the DNA solution, the same level of fluorescence quenching was reached as with the original order of adding the DNA to the liposomes.

3.3. Effect of solvent (H_2O versus D_2O) on TMADPH quenching

To determine whether the changes in fluorescence intensity of the fluorophore are induced by solvent relaxation [30], we compared the effects of H_2O (high solvent relaxation effect) to those of D_2O (low solvent relaxation effect) [31,32]. TMADPH-labeled liposomes were prepared either in H_2O or in D_2O, as described in Section 2. Complexes were formed by adding DNA to the same medium of the liposomes.

At $DNA^-/L^+ < 0.6$ (range 0–0.44) (Fig. 3, bottom), the level of fluorescence quenching in H_2O was high and similar to that in the low ionic strength Hepes buffer. A much lower level of fluorescence quenching ($\sim 30\%$) was obtained after complex formation in D_2O. At $DNA^-/L^+ \geq 1$ (Fig. 3, top) in H_2O, a significant increase in the fluorescence intensity occurred, similar to the one observed in low ionic strength Hepes buffer, which reached a plateau over the complete range of DNA^-/L^+. On the other hand, no increase in fluorescence intensity, and even some quenching, was measured in D_2O (Fig. 3, top). In contrast to TMADPH, the DPH fluorescence intensities of the DNA/DOTAP/DOPE complexes were similar in the H_2O and D_2O media (data not shown).

These data support the hypothesis that DNA interaction with cationic liposomes modifies the exposure of TMADPH (and, much less, of DPH) to water.

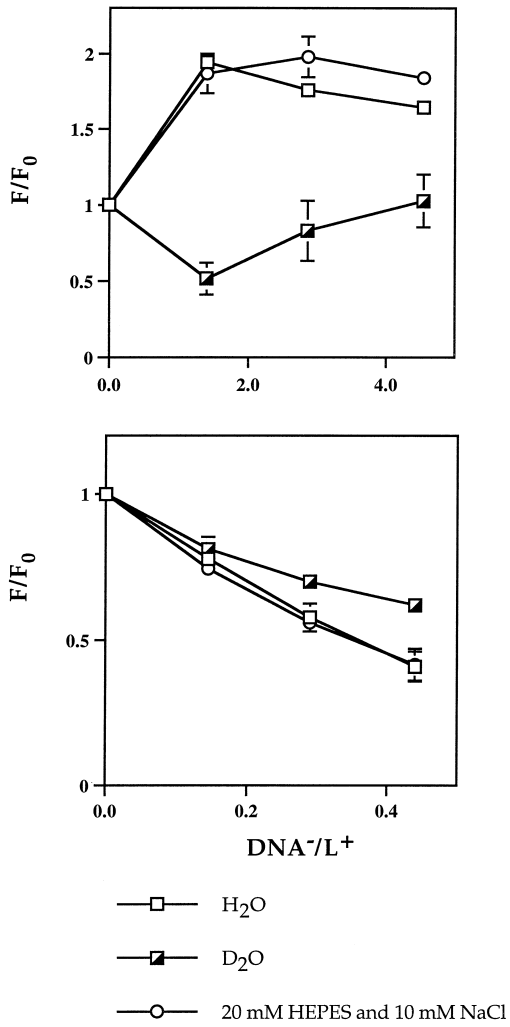

Fig. 3. Effect of H_2O and D_2O on formation of DOTAP/DOPE/DNA complexes as determined by relative fluorescence intensity of the probe TMADPH at the mole charge ratio of DNA^-/L^+ in the range < 0.6 (bottom), at which the lipid concentration was 0.78 mM; and at DNA^-/L^+ in the range ≥ 1 (top), at which the lipid concentration was 0.08 mM. Each point has a SD which can be observed only when the value is large enough to be visible.

3.4. TMADPH steady-state fluorescence anisotropy

The steady-state fluorescence anisotropy of TMADPH at room temperature in the cationic DOTAP/DOPE liposomes ($r = 0.206$) was compared to that of DOTAP/DOPE/DNA complexes; in the range of $DNA^-/L^+ < 0.6$ (ratio = 0.44), r was 0.345, and at $DNA^-/L^+ > 1$ (ratio $= 5.7$), r was 0.245.

These results suggest that the largest restriction to TMADPH rotation occurred at $DNA^-/L^+ < 0.6$, reaching a value close to the r_0 of TMADPH [32].

3.5. Fluorescence microscopy and freeze-fracture electron microscopy

The Noran confocal microscope (Noran Instruments, Middleton, WI) showed a very heterogeneous size distribution of the DNA–lipid ($DNA^-/L^+ = 0.44$) complexes in the range of light microscopy resolution (0.25–5.0 μm). Each large complex is actually a cluster of smaller fluorescent homogeneously labeled particles which are separated from each other by a dark (non-fluorescent) border (Fig. 4(a)).

The freeze-fracture electron micrograph (Fig. 4(b)) performed by Dr. B. Papahadjopoulos-Sternberg [33], indicates that each of these large (μm range) complexes is actually a cluster of closely packed particles (which may be partially fused), as was observed before for DNA/(DC-Chol/DOPE) in excess of lipids (Fig. 1 and Fig. 2 in [33]). For technical reasons, plasmid DNA in the complexes was not visible.

3.6. Size changes by PCS and specific turbidity

PCS measurements in DNA-containing systems may be misleading as they don't obey some of the

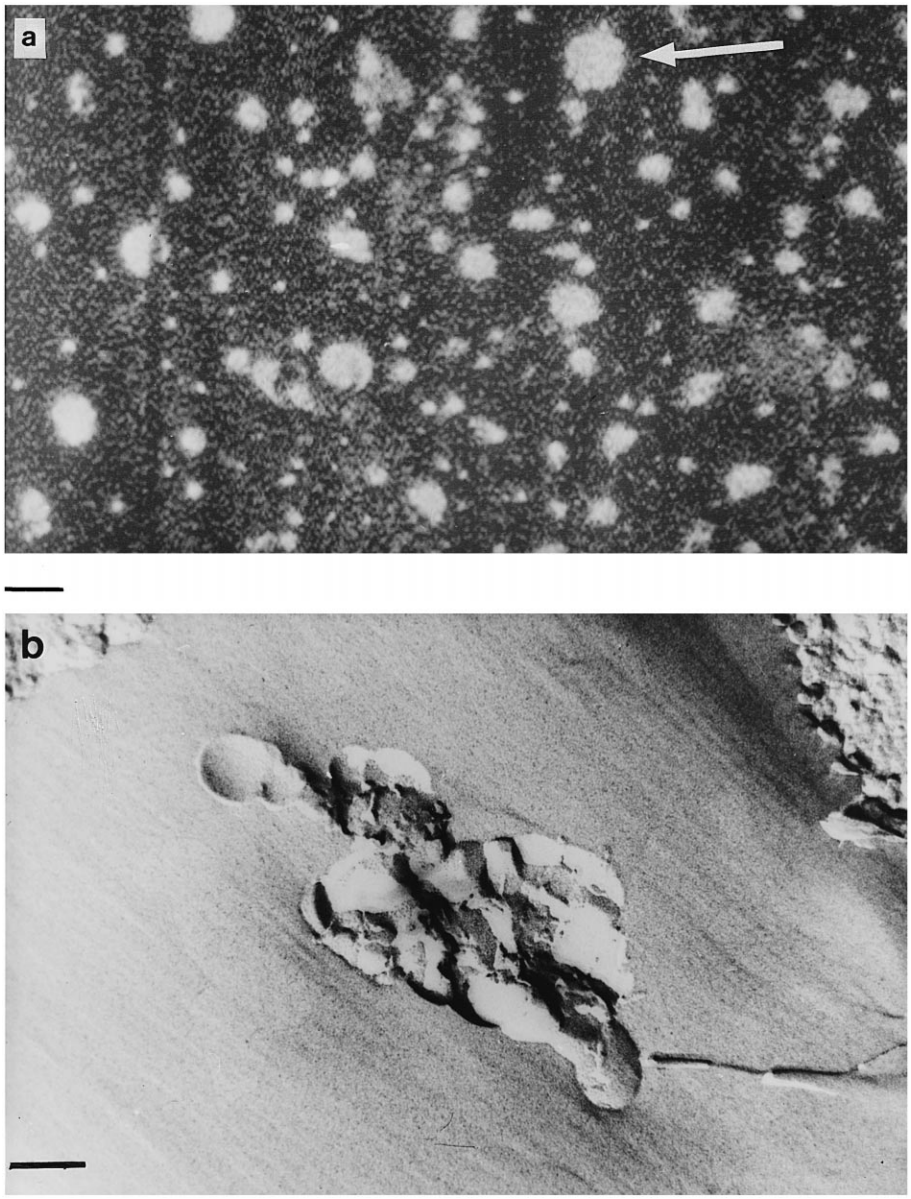

Fig. 4. (a) Confocal fluorescence micrograph of the TMADPH-labeled DNA–lipid complexes at the ratio of $DNA^-/L^+ = 0.44$. Scale bar represents 2 μm (see arrow). (b) Freeze-fracture electron micrograph of a DNA–lipid complex at $DNA^-/L^+ = 0.5$. Scale bar represents 100 nm.

basic rules of size determination by PCS [34] because there is a complex polymorphism in shape, size, and possibly composition [8,33], as well as hindered particle motion [35]. Also, the possible large contribution of DNA internal motion [36] makes the straightforward determination of size distribution by PCS questionable. Therefore we used PCS mainly to compare with the results of others, and we added the measurements of specific turbidity [36] as a more informative parameter. Specific turbidity reflects all the size changes in the system, including number of particles, size of particles, and changes in the refractive index. The two types of measurements agreed qualitatively but not quantitatively (Table 2). A very large increase in size (by both methods) occurred at $DNA^-/L^+ = 0.44$, and small or no change (specific

turbidity and PCS, respectively) occurred at $DNA^-/L^+ > 1$. The latter may be explained by changes in the refractive index due to the DNA–lipid complexation, with minimal changes in the particle size or the number of particles.

The same effects of DNA on size determination of the complexes by PCS and specific turbidity occurred in the presence and the absence of fluorophores (either TMADPH or DPH), indicating that the effect is directly related to the interaction of DNA with the cationic liposomes.

4. Discussion

4.1. General

Major questions in cationic lipid mediated lipofection are whether and how the physical properties of the DNA–lipid complexes affect transfection efficiency. Many of these physical properties (complex size, charge, hydration, and stability) are strongly related to the DNA^-/L^+ charge ratio. This study was aimed at characterizing changes in lateral organization of lipid molecules in the complexes, and in size of DNA–cationic lipid complexes. In two other studies [37,38] we characterized the electrostatic properties and stability of the cationic liposomes and the lipid–DNA complexes described here. The data presented here include the characterization of DNA^-/L^+ ratio related changes in fluorescence intensity and anisotropy of the fluorescent probes TMADPH and DPH embedded in the lipid assemblies, as well as size changes (PCS and specific turbidity measurements). Both types of fluorescence measurements and the two monitors of size agree and indicate major differences in properties between complexes formed at $DNA^-/L^+ < 0.6$ and $DNA^-/L^+ > 1$.

4.2. Size, TMADPH, and DPH fluorescence changes upon DNA–lipid interaction

The fluorescent probe TMADPH was chosen because its positively-charged quaternary amine resides close to the lipid/water interface, with the fluorophore aligned parallel to the upper part of the acyl chain [39]. Its fluorescence yield (but not spectrum) is sensitive to the polarity of the environment [22,31,40].

Our data suggest that TMADPH senses changes in the organization of the lipid assembly in the region which is close to the lipid/water interface. We hypothesized and tested that these changes in the fluorescence are related to degree of solvent relaxation due to the exposure of the fluorophores to water, as previously reported for similar systems [31]. The degree of exposure to water seems to be related to DNA^-/L^+ and to the location of the fluorophore in the lipid assembly. At ratios < 0.6 the fluorescence intensity of TMADPH is quenched, suggesting an increase in the fluorophore exposure to water, while at ratios ≥ 1 the fluorescence intensity is increased over that in the cationic liposomes lacking DNA, suggesting a reduction in the exposure to water molecules (Fig. 1). These results were unaffected by the low salt concentration (Fig. 3). However at 150 mM NaCl, TMADPH fluorescence was much smaller than at lower NaCl concentration (data not shown). The effect of NaCl supports the important role of electrostatics in complex formation [41].

The level of hydration at the lipid/water interface is related to the properties of the lipid headgroup region. Therefore the basic geometry of the three molecules (DOTAP, DOPC, and DOPE) was compared; each has two identical acyl chains (oleoyl chains), thus the differences between the three are related to the differences in their headgroups. Fig. 5 shows a space-filling model of the three lipids after free energy minimization (using CSC Chem3D/Plus software, Cambridge, MA). This figure clearly demonstrates that the headgroup area is in the order DOPC > DOPE > DOTAP. The packing parameter is defined as the ratio of the cross section of the hydrophobic region of the molecule to its polar headgroup area at the lipid/water interface [42]. However, other parameters which relate to the intermolecular interactions should also be considered. For these three molecules, hydrogen bonding at the headgroup region and its effect on the headgroup hydration are very important. Weaker hydration was observed for PEs and PC/PE systems, which was explained by the network of highly stable hydrogen bonds between the primary amino group of PE and the phosphate groups of either neighbor PC or PE molecules [43,44]. As the phosphate diester group in PC is responsible

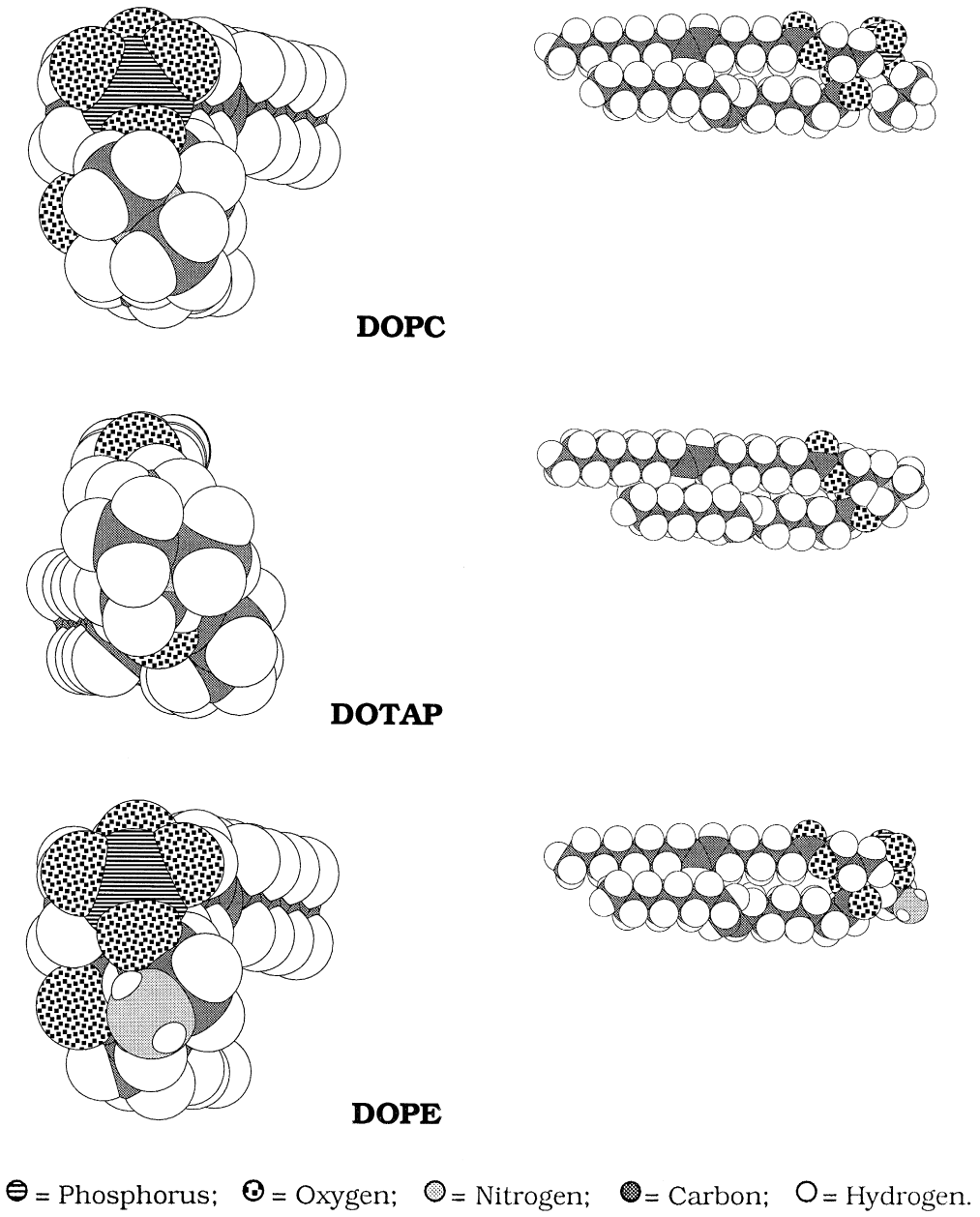

Fig. 5. Space-filling models of the molecules DOTAP, DOPE, and DOPC viewed from the headgroup side (left) and from the lateral plane (right). For more details see text.

for most of the PC hydration [43], this hydrogen bond capability, together with the relatively small headgroup, explains the unique polymorphism of hydrated lipid assemblies containing PE [45].

Based on the above considerations and the basic characterization data in Table 1, it is expected that DOTAP/DOPC and DOTAP/DOPE interfaces will be more hydrated than the DOPC/DOPE interface. Indeed, this is supported by the TMADPH specific fluorescence intensity, which is the highest in DOPC/DOPE vesicles (Table 1). A similar approach was used to demonstrate that cholesterol when present in PC vesicles reduces the level of surface hydration as assessed by the increase in quantum

yield of TMADPH present in the lipid bilayer upon the addition of cholesterol [31].

Polymorphism of the DNA–lipid complex population (concerning size and shape) was shown using electron microscopy [8,18,33]; it was also confirmed using fluorescence microscopy (Fig. 4). This heterogeneity was claimed as one of the major obstacles to optimize the efficacy of lipofection. The polymorphism can be partly due to the different hydration levels of the DNA–lipid complexes [8].

The effect of DNA on the fluorescence intensity of DPH in the same system was much smaller (on the quenching) at $DNA^-/L^+ < 0.6$ or none (on the enhancement) at $DNA^-/L^+ \geq 1$ (Fig. 1). Therefore, the DNA affects mainly the lipid/water interface region near the fluorophore. This is explained by the different location of these two probes in the lipid bilayer. As DPH has no polar group, it is located deeper in the hydrophobic region of the liposome membrane, either parallel to the lipid acyl chains or perpendicular to it between the two lipid monolayers [22,40]. Therefore, DPH is less exposed to the water molecules. The binding of DNA to the cationic lipids is electrostatic, involving the quaternary amino group of the cationic lipid and the negatively-charged phosphate of DNA [19]. Consequently, TMADPH, being a positively-charged amphiphile, is closer to DNA than DPH. The fact that TMADPH is much more affected than DPH indicates that the DNA interaction with the cationic lipid affects mainly the region close to the lipid–water interface. The validity of this approach was supported by the data showing that the addition of DNA has no effect on the fluorescence intensity when DOPC/DOPE liposomes labeled with TMADPH were used. This suggests that the affinity of TMADPH to lipids is much higher than to DNA; therefore the effect of equilibrium distribution [46] of TMADPH between the lipid environment and the DNA can be ruled out. In addition, the fact that the relationship between TMADPH fluorescence intensity and DNA^-/L^+ ratio is biphasic (quenching and enhancement) argues against a direct interaction of the DNA with the probe TMADPH.

Further support for our hypothesis on DNA changing the exposure to water of TMADPH present in the lipid bilayer follows from the experiments comparing the effect of H_2O versus D_2O on TMADPH fluorescence intensity. The fluorescence intensities of TMADPH and DPH are quenched due to solvent relaxation processes, which are most pronounced in H_2O [32] because of its large dipole moment which lowers the excited-state energy. Therefore, any agent or medium which will affect H_2O level at the location of the fluorophore, will induce changes in the total fluorescence intensity: Lowering the exposure of the fluorophore to water increases intensity, while increasing the exposure, decreases intensity. Replacing H_2O with D_2O, which has a lower solvent relaxation effect, should have a similar effect. Indeed, replacing H_2O by D_2O reduced the changes in TMADPH fluorescence intensity upon lipid–DNA complexing in all ranges of DNA^-/L^+ ratios (Fig. 3). The ratio of quantum yield $(F/F_0)H_2O/(F/F_0)D_2O$ can be used as a semi-quantitative measure of the exposure of the fluorophore to water. The lower the ratio, the higher the exposure to water. This method was used to show that cholesterol lowers the hydration level at the lipid/water interface [31]. The effect of D_2O supports the involvement of major changes in the exposure to water of the lipid region close to the lipid/water interface during DNA–lipid complexation.

DNA interaction with cationic liposomes induces a restriction in TMADPH motion, suggesting an increase in the packing density of the lipid acyl chains near the lipid/water interface in lipid domains which interact with the DNA. The DNA effect is much stronger at $DNA^-/L^+ < 0.6$; at this ratio range the fluorescence anisotropy r reaches a value close to the TMADPH r_0 of 0.379 [32]. Lifetime measurements (data not shown) indicate that these changes cannot be accounted for by changes in lifetime. The neutral helper lipid also has an effect, as the TMADPH specific fluorescence intensity (F_0) for DOTAP/DOPE > DOTAP/DOPC. This may be related to the fact that PE is less hydrated than PC [43]. The distribution of the fluorescence density between large and small complexes and across each particle, as visualized by confocal fluorescence microscopy (Fig. 4(a)) suggests a homogeneous distribution of TMADPH molecules at the resolution of UV light microscopy. However, from the information we have so far we cannot rule out DNA-induced phase separation between cationic lipid-rich domains containing the TMADPH and DOPE-rich hexagonal (Type II) domains at sub-light-microscopy resolution. Freeze-

fracture electron microscopy (Fig. 4(b)) and surface potential measurements (Fig. 5 in [38]) do not support such phase separation.

The largest changes in size, as monitored by both PCS and specific turbidity measurements, occur at $DNA^-/L^+ < 1$. Recently we also observed that at this ratio (but not at $DNA^-/L^+ > 1$), the process of size increase continues for many hours, leading to the formation of very large aggregates. Such a continuous process does not occur at $DNA^-/L^+ > 1$ [38]. Fluorescence microscopy of these TMADPH-labeled heterogeneous complexes reveals that every large complex is actually a cluster of tightly aggregated smaller particles which are separated by a thin non-fluorescent border. The exact nature of the smaller particles and the location of the DNA in these complexes is now under investigation.

4.3. Mechanism of DNA–cationic liposome interaction

All the above data on changes in fluorescence intensity, fluorescence anisotropy, fluorescence microscopy, and size distribution suggest the following mechanism: DNA condenses the lipids at the region close to the lipid/water interface by interacting with cationic lipid headgroups. This condensing effect is more pronounced at $DNA^-/L^+ < 0.6$ ($r = 0.345$). In this ratio range, the cationic lipid is only partially neutralized; e.g., at the ratio of 0.44, only 25% neutralization was achieved [38]. The amount of DNA is not sufficient to interact with and neutralize all the cationic lipids, even if the DNA is fully expanded. In addition, it is also known that at a certain level of charge neutralization DNA molecules exhibit packed shapes [47]. This fits well with the model of Dan [48]: DNA adsorbed to the surface of the cationic membrane at low DNA^-/L^+ induces formation of ordered domains in the bilayer (isothermal phase separation, Fig. 6), thereby perturbing the equilibrium packing of the lipids. At these ordered regions, the condensation of lipids at the upper part of the acyl chain region occurs. Packing defects at the edge of the ordered domain increase the level of water at the upper part of the bilayer acyl chains, causing TMADPH (but not DPH) to be quenched. The exposure to water of hydrophobic regions of the bilayer

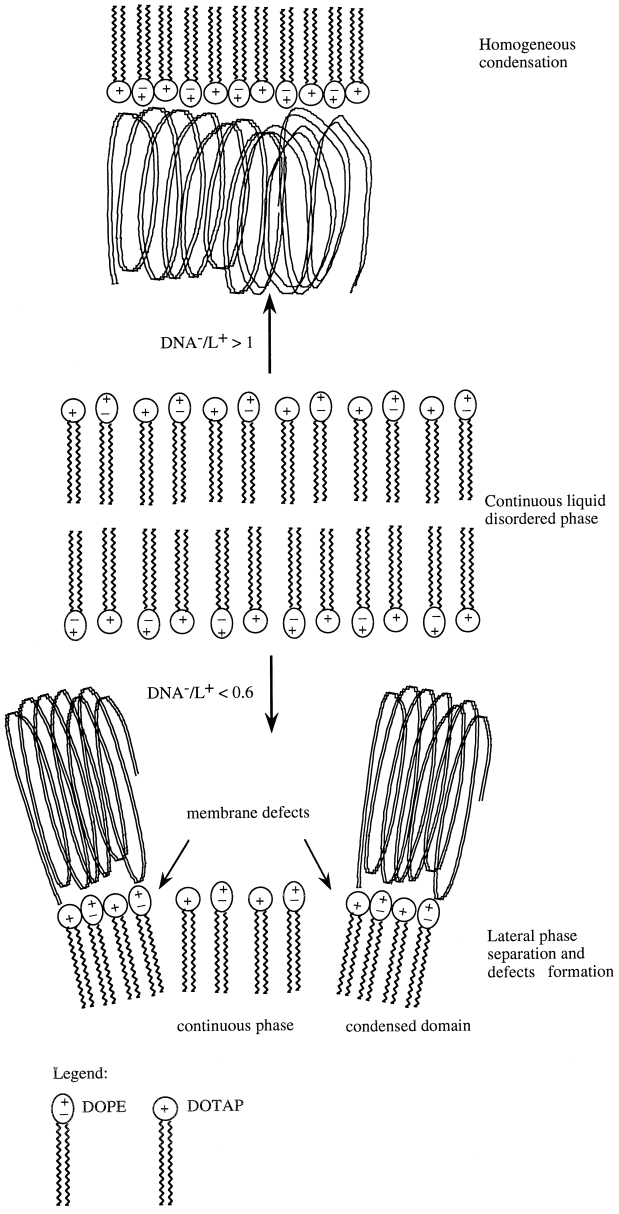

Fig. 6. Cartoon describing the effect of DNA on the lateral organization of the lipid bilayer (DOTAP/DOPE 1/1) at DNA^-/L^+ ratio of >1; 0; <0.6.

(which may be asymmetric by being limited to the external leaflet of the vesicle) may also explain the increase in size and possibly the fusion and lipid mixing observed by various investigators [7,17,18]. This may also explain the size and shape heterogeneity of the complexes, exemplified by Zabner et al. [8], using negative staining rotatory shadowing electron microscopy, by Gustafsson et al. [49], using cryo-

TEM, and by us, using fluorescence microscopy of TMADPH-labeled complexes (Fig. 4(a)). The latter studies suggest that an excess of positively-charged lipids leads to entrapment of DNA between the lamellae in clusters of aggregated multilamellar structures (see also Fig. 4(b)). Such an organization was also supported by recent X-ray scattering studies [35], by our own measurements on the electrostatic properties and size/structure of the complexes [38], and by small-angle X-ray-scattering and cryo-TEM [49,50]. The extremely high increase in TMADPH fluorescence anisotropy may be explained by the faster lateral mobility of the positively-charged probe relative to the diacyl lipids, which may lead to its concentration at the domains of lipid–DNA interaction. This uneven distribution (if it exists) is limited to the submicron scale, as it was not observed by the confocal fluorescence microscopy of TMADPH-labeled complexes (Fig. 4(a)).

At ratios of $DNA^-/L^+ > 1$, more lipid molecules interact with the DNA, and the level of cationic lipid neutralization is much higher. We found that the maximum and constant level of neutralization (80% for the DOTAP/DOPE system [37]) occurs at $DNA^-/L^+ \geq 1$. The condensing effect at the upper part of the lipid bilayer, although occurring, is much smaller ($r = 0.245$). Actually, there is no formation of ordered domains and therefore no packing defects in the membrane plane, as all the surface interacts homogeneously with the DNA (Fig. 6). This leads to a reduction in the exposure of hydrophobic regions to water at this ratio range. The lack of defects in the lipid bilayer is also supported by the fact that no, or only minimal, changes in size (monitored by PCS or turbidity, respectively) occurred at $DNA^-/L^+ \geq 1$. That is, the complexes formed at ratios of $DNA^-/L^+ < 0.6$ and ≥ 1 differ largely in their structure at both the molecular and macroscopic levels. The relevance of these finding to the transfection process in vitro and in vivo is now under investigation.

Acknowledgements

This study was supported in part by Israel Science Foundation grant 494/96 to Y.B. The authors wish to thank Dr. Nili Dan of the Department of Chemical Engineering, University of Delaware, Newark, DE, and Dr. Danilo D. Lasic, Liposome Consultations, Newark, CA, for sharing their manuscripts prior to publication; Dr. Y. Talmon and Ms. M. Goldraich of the Department of Chemical Engineering, Technion, Haifa, Israel, for the cryo-TEM of cationic liposomes; Dr. B. Papahadjopoulos-Sternberg of the Institute of Ultrastructure Research, Medical School, Friedrich-Schiller-University Jena, Jena, Germany for performing freeze-fracture electron microscopy; Dr. O. Meyuhas of our department for the S16 hGH plasmid; and Mr. S. Geller for help in editing the manuscript.

References

[1] P.L. Felgner, T.R. Gadeck, M. Holm, R. Roman, H.W. Chan, M. Wenz, J.P. Northrop, G.M. Ringold, M. Danielsen, Proc. Natl. Acad. Sci. U.S.A. 84 (1987) 7413–7417.
[2] J.P. Behr, B. Demeneix, J.-P. Loeffler, J. Perez-Mutul, Proc. Natl. Acad. Sci. U.S.A. 86 (1989) 6982–6986.
[3] R. Leventis, J.R. Silvius, Biochim. Biophys. Acta 1023 (1990) 124–132.
[4] X. Gao, L. Huang, Biochem. Biophys. Res. Commun. 179 (1991) 280–285.
[5] H. Farhood, R. Bottega, R.M. Epand, L. Huang, Biochim. Biophys. Acta 1111 (1992) 239–246.
[6] X. Zhou, L. Huang, Biochim. Biophys. Acta 1189 (1994) 195–203.
[7] P.L. Felgner, Y.J. Tsai, J.H. Felgner, in: D.D. Lasic, Y. Barenholz (Eds.), Handbook of Nonmedical Applications of Liposomes, CRC Press, Boca Raton, FL, vol. 4, chap. 4, 1996, pp. 43–56.
[8] J. Zabner, A.J. Fasbender, T. Moninger, K.A. Poellinger, M.J. Welsh, J. Biol. Chem. 270 (1995) 18997–19007.
[9] P.L. Felgner, G.M. Ringold, Nature 337 (1989) 387–388.
[10] K. Goyal, L. Huang, J. Liposome Res. 5 (1995) 49–60.
[11] S. Capaccioli, G. Di Pasquale, E. Mini, T. Mazzei, A. Quattrone, Biochem. Biophys. Res. Commun. 197 (1993) 818–825.
[12] G. McLachlan, D.J. Davidson, B.J. Stevenson, P. Dickinson, H. Davidson-Smith, J.R. Dorin, D.J. Porteous, Gene 2 (1995) 614–622.
[13] J.G. Pickering, J. Jekanowski, L. Weir, S. Takeshita, D.W. Losordo, J.M. Isner, Circulation 89 (1994) 13–21.
[14] H. San, Z.Y. Yang, V.J. Pompili et al., Hum. Gene Ther. 4 (1993) 781–788.
[15] J.H. Felgner, R. Kumar, S.H. Sridhar, C.J. Wheeler, Y.J. Tsai, R. Border, P. Ramsey, M. Martin, P.L. Felgner, J. Biol. Chem. 269 (1994) 2550–2561.

[16] A. Minsky, R. Ghirlando, H. Gershon, in: D.D. Lasic, Y. Barenholz (Eds.), Handbook of Nonmedical Applications of Liposomes, CRC Press, Boca Raton, FL, vol. 4, Chap. 2, 1996, pp. 7–30.
[17] H. Gershon, R. Ghirlando, S.B. Guttman, A. Minsky, Biochemistry 32 (1993) 7143–7151.
[18] S.J. Eastman, C. Siegel, J. Tousignant, A.E. Smith, R.K. Cheng, R.K. Scheule, Biochim. Biophys. Acta 1325 (1997) 41–62.
[19] Y. Barenholz, S. Amselem, in: G. Gregoriadis (Ed.), Liposome Technology, Liposome Preparation and Related Techniques, 2nd ed, CRC Press, Boca Raton, FL, vol. 1, 1993, pp. 527–616.
[20] S. Levy, D. Avni, N. Hariharan, R.P. Perry, O. Meyuhas, Proc. Natl. Acad. Sci. U.S.A. 88 (1991) 3319–3323.
[21] R.C. MacDonald, R.I. MacDonald, B.P.M. Menco, K. Takeshita, N.K. Subbarao, L. Hu, Biochim. Biophys. Acta 1061 (1991) 297–303.
[22] V. Borenstain, Y. Barenholz, Chem. Phys. Lipids 64 (1993) 117–127.
[23] Y. Talmon, Ber. Bunsenges. Phys. Chem. 100 (1996) 364–372.
[24] Y. Barenholz, E. Freire, T.E. Thompson, M.C. Correa-Freire, D. Bach, I.R. Miller, Biochemistry 22 (1983) 3497–3501.
[25] D.G. Cameron, E.F. Gudgin, H.H. Mansch, Biochemistry 20 (1981) 4496–4500.
[26] B. Pullman, A. Pullman, H. Berthod, N. Gresh, Theor. Chim. Acta (Berl.) 40 (1975) 93–111.
[27] Y. Katz, J.M. Diamond, J. Membr. Biol. 17 (1974) 69–154.
[28] R. Pal, W.A. Petri, V. Ben-Yashar, R.R. Wagner, Y. Barenholz, Biochemistry 24 (1985) 573–581.
[29] E.G. Nabel, Z. Yang, S. Liptay, H. San, D. Gordon, C.C. Haudenschild, G.J. Nabel, J. Clin. Invest. 91 (1993) 1822–1829.
[30] L. Stryer, J. Am. Chem. Soc. 88 (1966) 5708–5712.
[31] C. Ho, C.D. Stubbs, Biophys. J. 63 (1992) 897–902.
[32] J.R. Lacowicz, Principles of Fluorescence Spectroscopy, Plenum Press, New York, 1983.
[33] B. Sternberg, F.L. Sorgi, L. Huang, FEBS Lett. 356 (1994) 361–366.
[34] N. Ostrovsky, Chem. Phys. Lipids 64 (1993) 45–56.
[35] J.O. Radler, I. Koltover, T. Salditt, C.R. Safinya, Science 275 (1997) 810–814.
[36] J. Langowski, W. Kermer, U. Kapp, Methods Enzymol. 11 (1992) 430–448.
[37] N.J. Zuidam, Y. Barenholz, Biochim. Biophys. Acta 1329 (1997) 211–222.
[38] N.J. Zuidam, Y. Barenholz, Biochim. Biophys. Acta (1998) in press.
[39] V. Ben-Yashar, Y. Barenholz, Chem. Phys. Lipids 60 (1991) 1–14.
[40] B.R. Lentz, Chem. Phys. Lipids 50 (1989) 171–190.
[41] D.D. Lasic, Liposomes in Gene Delivery, CRC Press, Boca Raton, FL, 1997.
[42] J.N. Israelachvili, Intermolecular and Surface Forces, 2nd ed. Academic Press, London, 1991.
[43] D.W.R. Gruen, S. Marcelja, V.A. Parsegian, in: A.S. Perelson, C. DeLisi, F.W. Wiegel (Eds.), Cell Surface Dynamics: Concepts and Models, Marcel Dekker, New York, Chap. 3, 1984, pp. 59–91.
[44] J. Wilschut, D. Hoekstra, Chem. Phys. Lipids 40 (1986) 145–166.
[45] D.C. Litzinger, L. Huang, Biochim. Biophys. Acta 1113 (1992) 201–227.
[46] M. Shinitzky, Y. Barenholz, Biochim. Biophys. Acta 515 (1978) 367–394.
[47] G.S. Manning, Biopolymers 19 (1980) 37–59.
[48] N. Dan, Biophys. J. 71 (1996) 1267–1272.
[49] J. Gustafsson, G. Arvidson, G. Kalsson, M. Almgren, Biochim. Biophys. Acta 1235 (1995) 305–312.
[50] D.D. Lasic, H. Strey, M.C.A. Stuart, R. Podgornick, P.M. Fredrick, J. Am. Chem. Soc. 119 (1997) 832–833.